AD NUMBER

AD044222

LIMITATION CHANGES

TO:

Approved for public release; distribution is unlimited.

FROM:

**Distribution authorized to U.S. Gov't. agencies and their contractors;
Administrative/Operational Use; SEP 1953. Other requests shall be referred to Office of Naval Research, Washington, DC 20360.**

AUTHORITY

onr d/n ltr, 26 oct 1972

D

44222

UNCLASSIFIED

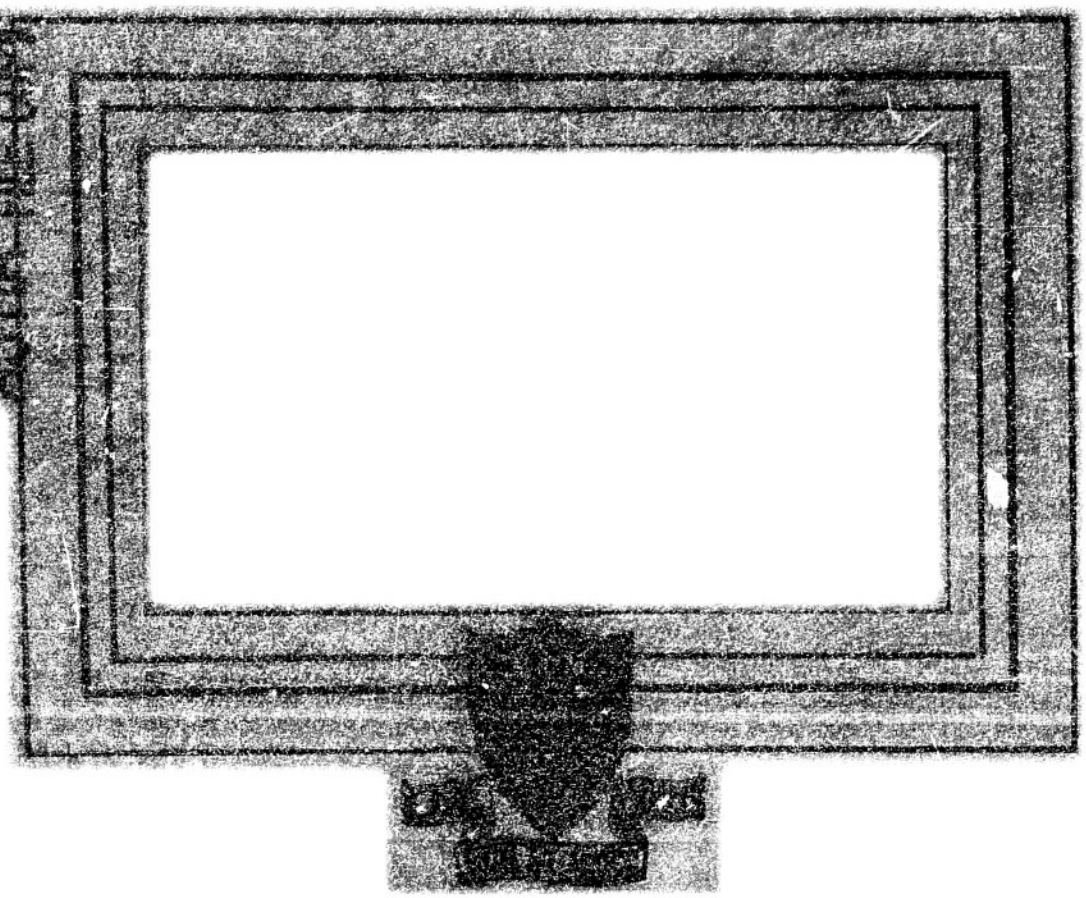

RESEARCH BULLETIN

THE JAMES FORRESTAL RESEARCH CENTER
PRINCETON UNIVERSITY

THE MIXING OF AN AXIALLY SYMMETRIC COMPRESSIBLE JET WITH QUIESCENT AIR

by

Walter R. Warren, Jr.

Aeronautical Engineering Laboratory Report No. 252

September 30, 1953

A Research Report Submitted to the Department of Aeronautical Engineering in Partial Fulfillment of the Requirements of the Doctor of Philosophy Degree.

PRINCETON UNIVERSITY

Princeton, New Jersey

ACKNOWLEDGEMENT

This study was conducted in connection with Contract PR-N6 ori-105, Task Order III, for Project SQUID, which is a cooperative research project in jet propulsion under the sponsorship of the Office of Naval Research, Department of the Navy; the Research and Development Command, Department of the Air Force; and the Office of Ordnance Research, Department of the Army. The author acknowledges with thanks the sponsorship of this work.

Abstract

A semi-empirical theory is presented for predicting the boundaries, velocity decay on the axis, and the velocity at any point in an air jet or variable density exhausting into air at rest.

The integrated axial momentum equation is employed as the basic equation in the analysis and an approximate expression for density variation is presented and analyzed. The shear stress is represented by a form suggested by Reichardt. This form is simpler than the ordinary Prandtl expression.

Calculations are made for range of density ratios and an analysis of the results is attempted.

A comparison with experiment is made indicating that the mixing parameter $\frac{k}{u_1}$ is dependent upon the density ratio.

A method for solution of the mixing problem using a more exact density variation is indicated in Appendix I.

TABLE OF CONTENTS

SYMBOLS

x	Distance along jet axis
r	Radial distance from jet axis
ρ	Density
p	Pressure
T	Temperature
a	Speed of sound
u	Velocity in x direction
M	Mach number, u/a
γ	Ratio of specific heats
k	Shear stress proportionality factor
$\frac{k}{u_1}$	Mixing parameter
τ	Shear stress
e	Turbulent viscosity coefficient
ϵ	Turbulent kinematic viscosity coefficient
δx	Differential x distance
m_t	Total jet momentum flux
m	Momentum flux constant
R	Dimensionless radius, r/r_1
X	Dimensionless axial distance, x/r_1
U	Dimensionless velocity, u/u_1
X_c	Axial length of potential core

SUBSCRIPTS

1	Jet exit conditions
a	Quiescent air conditions
*	Integration limit conditions in integral equation
i	Potential core boundary
o	Outer jet boundary

THE MIXING OF AN AXIALLY SYMMETRIC COMPRESSIBLE JET WITH QUIESCENT AIR

Introduction

The problem of the mixing of a turbulent jet with its surrounding medium has been analyzed extensively in recent years because of its obvious importance in many engineering applications and, also, because of its direct association with the problem of free turbulence.

In 1926, Tollmien(1) effectively initiated work in this field by extending an analysis of laminar jets to turbulent jets through the use of the Prandtl mixing length theory(2). His theory was applied to jets issuing from a point source. Since that time, many noteworthy analytical and experimental contributions have been made. Among these have been Kuethe's calculation(3), in 1935, of the velocity profile in the initial portion of a jet exhausting into a medium at rest; the suggestion by Reichardt(4), in 1941, of a new theory of free turbulence; the calculation of jet spread and velocity decay of a finite jet exhausting into a moving stream by Squire and Trouncer(5) in 1944; the experimental work of Forstall and Shapiro(6), reported in 1950; and the analytical and experimental analyses that have been in progress at the Engineering Experiment Station of the University of Illinois since 1948. A large percentage of the work that has been done, including those contributions mentioned above, deals only with incompressible flow. Although there have been a number of experimental investigations of compressible jets, the only theoretical approaches that are well known are those of Pai(7) and Szablewski(8).

In general, one of three approaches is used when a theoretical analysis of the problem is attempted. In the first approach, a solution

of the turbulent differential equations of motion is sought in order to determine the velocity profile as a function of axial distance. Kuethe, for the incompressible case, and both Pai and Szablewski, for the compressible case, followed this method. Kuethe found an approximate solution to his equation using the Prandtl mixing length theory expression for the turbulent shear stress. Pai reduced the turbulent equations to a solvable form after relating the turbulent fluctuations to the mean properties of the flow through Taylor's modified vorticity theory(2) and representing the density variation by a form of the Crocco energy integral. Szablewski assumed that a modified form of the Prandtl mixing length expression represented the shear stress and eliminated density from his momentum equation by assuming that the apparent turbulent viscosity coefficient divided by the density was constant with respect to the radial dimension. A major difficulty arising in this type of treatment is obtaining a solution of the equations which are always non-linear. A small perturbation analysis will usually linearize the equations for small density and velocity variations and reduce the solution difficulties. However, large variations invariably necessitate the use of highly involved numerical methods of solution.

The second approach is one which uses an integrated momentum equation of the Karman type(2). In this type of analysis, velocity profiles must be assumed to be similar throughout the jet or at least in portions that are treated separately, and a particular velocity profile shape must be assumed in order to solve the resulting equations. Squire and Trouncer used this method, representing the shear stress by the Prandtl form, to calculate the spread of the jet and the velocity decay along the axis for the case of incompressible mixing

between a jet and a moving external stream. Their calculations were much simpler than those arising from the use of the ordinary differential equations, and their assumptions regarding the shape and similarity of velocity profiles were well verified by Forstall and Shapiro.

The third method that has been used is based upon Reichardt's theory of free turbulence. Essentially, Reichardt replaces the gradient, or conductive, mechanism of momentum transfer by a diffusion process, thus discarding the basis upon which the Prandtl expression for shear stress is derived. Some experimental verification of Reichardt's hypothesis has been achieved; for example, Kivnick(9), at the University of Illinois has fitted the data of Forstall and Shapiro to an analysis of the Reichardt type reasonably well.

It should be realized that these analyses of turbulent jet mixing can only be classified as semi-empirical theories because of the unknown constants that always appear in the results. These constants result from the rather arbitrary representation of the turbulent shear stress and must be evaluated experimentally.

It is the object of this paper to include the effects of compressibility in the mixing problem by a method that will allow solution without a prohibitive amount of calculation. The velocity of the outside stream is taken as zero to simplify the problem and, also, because the experimental equipment at this laboratory can be easily adapted to such a condition.

A method similar to that used by Squire and Trouncer is employed. The effect of density variation is accounted for by an approximation that assumes the density at any point in the jet is a particular function of the local mean velocity and constant quantities only. Because it is

believed to be not valid in compressible flow, the usual Prandtl representation of shear stress is discarded. A somewhat simpler form, similar to that suggested by Reichardt, is used.

The transfer of mass and energy are not treated, since experimental results, particularly those of Townsend(10), indicate that the mechanism of transport for these quantities in a free turbulence phenomena is different from that for momentum. Therefore, it does not seem logical to present similar analyses for the three quantities.

Theory

A. Derivation of Integral Equation

The integrated axial momentum equation(2) used in this analysis is

$$\frac{\partial}{\partial x}\int_0^{r_*} \rho u^2 r\,dr - u_* \frac{\partial}{\partial x}\int_0^{r_*} \rho u\, r\,dr = \tau r_* \tag{1}$$

A brief derivation will aid in the understanding of equation 1 and its subsequent use in the solution of the mixing problem.

Consider a circular disk of air, as shown in Figure 1, in a general steady flow which is symmetric with respect to the x axis. The change of axial momentum across the faces of the disk per unit time is

$$\delta x \cdot \int_0^{r_*} \frac{\partial(\rho u^2)}{\partial x} 2\pi r\,dr \tag{2}$$

The change of mass between the two faces of the disk per unit time is

$$\delta x \cdot \int_0^{r_*} \frac{\partial(\rho u)}{\partial x} 2\pi r\,dr$$

and, since this mass can only flow across the $r = r_*$ surface, the axial momentum change associated with the mass flow change is

$$u_* \cdot \delta x \cdot \int_0^{r_*} \frac{\partial(\rho u)}{\partial x} 2\pi r\,dr \tag{3}$$

The force exerted on the disk by the shear stress τ is

$$\delta x \cdot 2\pi r_* \cdot \tau \tag{4}$$

Notice the Expression 4 ignores the change in τ between x and $x + \delta x$ which is considered to be a second order effect. The pressure gradients in the r and x directions are assumed to be negligible, following the usual boundary layer and jet assumptions, thus causing no unbalanced pressure force on the disk.

A summation of forces acting on the disk of Figure 1 Expressions 2, 3, and 4, yields

$$\int_0^{r_*} \frac{\partial(\rho u^2)}{\partial x} r\,dr - u_* \int_0^{r_*} \frac{\partial(\rho u)}{\partial x} r\,dr = \tau r_* \qquad (5)$$

The signs of the terms in Equation 5 are dictated by the type of problem being investigated and the form that is to be used to represent the shear stress τ. Equation 5 can be transformed simply by Leibnitz's Rule to the form given in Equation 1.

B. Approach to Free Jet Analysis

The derivation of solvable equations in terms of unknown quantities used in this analysis is similar to that employed by Squire and Trouncer and will be discussed only briefly here. As shown in Figure 2, the jet is divided into two regions: the core region, in which a "potential" core of constant quantities exists; and the developed region, in which the core has disappeared and the properties of the jet are changing continuously with r and x. Notice that the mixing region boundaries, r_o and r_i, are defined by the spread of velocity, or momentum.

It is assumed then that similarity of velocity profiles exists in both regions and that these profiles can be represented by a cosine variation (see Figure 3).

Core region:

$$u = \frac{u_c}{2}\left\{1 - \cos\pi\left[\frac{r_o - r}{r_o - r_i}\right]\right\} \qquad (6)$$

Developed region:

$$u = \frac{u_c}{2}\left\{1 + \cos \pi \frac{r}{r_0}\right\} \tag{7}$$

This assumption is well verified by experiment in the incompressible case(6) and early experiments at this laboratory(11) indicate that such an assumption is still reasonably valid for an extremely cold jet. Notice that both Equation 6 and 7 become identical at the downstream limit of the potential core.

Now suppose that the density ρ and the shear stress τ can be represented as functions of u, r_c, and r_i. This will be discussed in the following sections. Then, in principle, the problem can be solved in the following manner:

Core Region

Evaluate Equation 1 at $r^* = r_0$:

$$\tau_{r=r_0} = 0 \quad ; \quad u_{r=r_0} = 0$$

Therefore, Equation 1 becomes

$$\frac{2}{\delta x}\int_0^{r_0} \rho u^2 r\, dr = 0$$

or

$$\int_0^{r_0} \rho u^2 r\, dr = \text{Const.} = m \tag{8}$$

Equation 8 expresses the condition of conservation of total momentum; i.e., the momentum at the jet exit which is $m_1 = \rho_1 u_1^2 \pi r_1^2$

will be equal to the total momentum integrated across the jet at any station x. Therefore, the constant M in Equation 8 can be evaluated immediately as

$$m = \frac{\rho_i u_i^2 r_i^2}{2} \tag{9}$$

Equation 8 can be reduced to a more usable form by splitting the integral into two parts

$$\int_0^{r_i} \rho u^2 r\, dr + \int_{r_i}^{r_o} \rho u^2 r\, dr = m \tag{10}$$

In Equation 10

$$\int_0^{r_i} \rho u^2 r\, dr = \rho_i u_i^2 \int_0^{r_i} r\, dr = \frac{\rho_i u_i^2 r_i^2}{2}$$

so that Equation 10 becomes

$$\frac{\rho_i u_i^2 r_i^2}{2} + \int_{r_i}^{r_o} \rho u^2 r\, dr = m \tag{11}$$

Evaluate Equation 1 at $r^* = \frac{r_o + r_i}{2}$:

$$\tau_{r^*=\frac{r_o+r_i}{2}} = \tau\left(\frac{u_i}{2}, r_i, r_o\right) \; ; \quad u_{*r_o=\frac{r_o+r_i}{2}} = \frac{u_i}{2}$$

therefore, Equation 1 becomes

$$\frac{\partial}{\partial x}\int_0^{\frac{r_o+r_i}{2}} \rho u^2 r\, dr - \frac{u_i}{2}\frac{\partial}{\partial x}\int_0^{\frac{r_o+r_i}{2}} \rho u r\, dr = \tau_{\frac{r_o+r_i}{2}} \cdot \frac{r_o+r_i}{2} \tag{12}$$

Again, by splitting the integrals, Equation 12 reduces to

$$\frac{\rho_i u_i^2}{4}\frac{\partial r_i^2}{\partial x} + \frac{\partial}{\partial x}\int_{r_i}^{\frac{r_o+r_i}{2}} \rho u^2 r\,dr - \frac{u_c}{2}\frac{\partial}{\partial x}\int_{r_i}^{\frac{r_o+r_i}{2}} \rho u r\,dr = \tau_{\frac{r_o+r_i}{2}} \cdot \frac{r_o+r_i}{2} \qquad (13)$$

According to the assumption above that ρ and τ may be expressed in terms of u, r_i, and r_o and that u is a known function of r, Equations 11 and 13 are recognized to be two simultaneous equations for the two unknowns, $r_i(x)$ and $r_o(x)$, and in principle, can be solved for these unknowns.

Developed Region

The derivation of equations in the developed region is similar to that in the core region. However, the unknown $u_c(x)$ now replaced the unknown $r_i(x)$.

Evaluate Equation 1 at $r^* = r_o$:

$$\tau_{r=r_o} = 0 \quad ; \quad u^*_{r=r_o} = 0$$

Then Equation 1 becomes

$$\frac{\partial}{\partial x}\int_0^{r_o} \rho u^2 r\,dr = 0$$

which expresses the same relationship as Equation 8. Therefore,

$$\int_0^{r_o} \rho u^2 r\,dr = m = \frac{\rho_i u_i^2 r_i^2}{2} \qquad (14)$$

r_o

Evaluate Equation 1 at $r^* = \frac{1}{2}$:

$$\tau_{r=\frac{r_o}{2}} = \tau\left(\frac{u_c}{2}, r_o\right) \quad ; \quad u^*_{r=\frac{r_o}{2}} = \frac{u_c}{2}$$

Equation 1 becomes

$$\frac{\partial}{\partial x}\int_0^{r_o/2} \rho u^2 r\,dr - \frac{u_c}{2}\frac{\partial}{\partial x}\int_0^{r_o/2} \rho u r\,dr = \tau_{\frac{r_o}{2}} \cdot \frac{r_o}{2} \qquad (15)$$

Equations 14 and 15 are two simultaneous equations for the two unknowns, $r_o(x)$ and $u_c(x)$.

It is seen now that the problem will be completely solved when $r_o(x)$, $r_i(x)$, and $u_c(x)$ are known, since the velocity profiles at any station x can be constructed by the use of Equation 6 or Equation 7.

C. Density Variation

As has been mentioned, the use of the two sets of simultaneous equations derived above for the solution of the problem depends upon the possibility of expressing the density ρ as a function of not more than the three variables u, r_o, and r_i. The special case of incompressible flow, ρ = constant, has been treated by Squire and Trouncer. In this paper, an attempt is made to solve the mixing problem for the general case of a jet of uniform initial density ρ_i which is arbitrarily different from the density ρ_a of the outside medium. It is necessary then to choose a suitable function to represent the variation of density.

Pai uses an expression of the Crocco type to satisfy the temperature variation in the mixing region of the free jet,

$$T = A + Bu - \frac{u^2}{2C_p}$$

The quantities A and B are constants that are determined by the boundary conditions of the problem. Since the pressure in the free jet is assumed to be constant, the density variation could be expressed as

$$\frac{1}{\rho} = f\left(A + Bu - \frac{u^2}{2C_p}\right) \frac{R}{p} \qquad (16)$$

or, in other words, the density variation is a function of velocity alone

and constant quantities. It was observed that the use of Expression 16 would cause great difficulty in the evaluation of the integrals in Equations 11, 13, 14, and 15 when Equations 6 and 7 were substituted for the velocity variation. Therefore, a different variation of density is used; however, its dependence upon velocity alone is retained. Appendix I presents a possible method for the inclusion of a variation of the type shown in Equation 16.

The density variation that was chosen is

$$\rho - \rho_a = c u^2 \tag{17}$$

The constant in Equation 17 is determined from the condition at the nozzle exit as

$$c = \frac{\rho_i - \rho_a}{u_i^2}$$

and, therefore, the density at any point of the mixing region is given by

$$\rho = \frac{\rho_i - \rho_a}{u_i^2} u^2 + \rho_a \tag{18}$$

It is realized that Equation 18 is only an approximation. An estimate of its validity can be made in the following manner:

Since p = constant, $\frac{T_a}{T} = \frac{\rho}{\rho_a}$ and $\frac{T_a}{T_i} = \frac{\rho_i}{\rho_a}$

Substitution into Equation 18 gives

$$\frac{T_a}{T} - 1 = \left(\frac{T_a}{T_i} - 1 \right) \frac{u^2}{u_i^2} \tag{19}$$

Now, if the special case in which the jet has the same stagnation enthalpy as the surrounding fluid is considered, $T_a = T_{s1}$, and

$$\frac{T_a}{T_1} = 1 + \frac{\gamma-1}{2} M_1^2$$

It is assumed that $T_a = T_s$ throughout the mixing region. Therefore Equation 19 becomes

$$\frac{T_a}{T} = 1 + \frac{\gamma-1}{2} M_1^2 \frac{u^2}{a_1^2}$$

or

$$\frac{T_a}{T} = 1 + \frac{\gamma-1}{2} \frac{u^2}{a_1^2} \qquad (20)$$

Equation 20 is similar to the ordinary expression for the adiabatic, one dimensional flow of a perfect gas

$$\frac{T_a}{T} = 1 + \frac{\gamma-1}{2} \frac{u^2}{a^2}$$

except that the constant a_1^2 is substituted for the variable (throughout the mixing region) a^2.

Consider a cold jet; i.e., one in which the temperature of the jet is less than the surrounding medium. The quantity $\frac{\gamma-1}{2} \frac{u^2}{a_1^2}$ will always be larger than $\frac{\gamma-1}{2} \frac{u^2}{a^2}$ as one goes away from the potential core because of the restriction placed upon a_1. The error will be small near the core and will increase as the distance from the core increases. However, as one goes away from the core, u^2 becomes very small and the contribution of the increased error in a_1^2 is believed to be small.

For a hot jet; i.e., one in which the temperature of the jet is

Greater than the surrounding medium; it is impossible to have the same stagnation enthalpy in both the jet and the external fluid, and the analysis does not apply.

Suppose that $\rho - \rho_a = C u^2$ had been used instead of Equation 17. The equation that is derived for the case of constant total enthalpy, corresponding to Equation 20 for the u^2 variation is,

$$\frac{T_a}{T} = 1 + \frac{\gamma - 1}{2} \frac{u_a^2}{a_1^2} \frac{u}{u_1} \tag{21}$$

In Equation 21, the term $\frac{u}{u_1}$ has a reducing effect upon the right side of the equation. For the cold jet, this is compensating compared to the u^2 variation, however, it should be noticed that the compensating effect for the cold jet will probably be too great at larger distances from the potential core since $\frac{u}{u_1} \to 0$.

If a density variation of the type $\rho - \rho_a = C u$ is used, the equation corresponding to Equation 20 is

$$\frac{T_a}{T} = 1 + \frac{\gamma - 1}{2} \frac{u_a^2}{a_1^2} \frac{1}{u_a/u_1} \tag{22}$$

The $\frac{1}{u_a/u_1}$ term in Equation 22 will add to the error for the cold jet.

Therefore, it is believed that, at least for a cold jet, the density variation can be represented by an expression of the form

$$\rho - \rho_a = C u^n$$

where n varies between 2 and 3 throughout the mixing region. For this analysis, the value of $n = 2$ was used. It is assumed that, at least for

a jet whose initial density is not radically different from that of the surrounding fluid, the density value given by Equation 8 will give a reasonable representation of the actual phenomena.

It should be mentioned that the density change represented by Equation 18 will satisfy the condition of a stream of arbitrary velocity so long as the assumptions of the analysis are not violated; for example, the presence of shock waves in the jet core would spoil the assumption of uniform velocity.

D. Shear Stress Representation

The representation of the shear stress in an analysis of a turbulent flow has been a controversial subject for many years. The most well-known method is that of the momentum transfer theory based upon the Prandtl mixing length theory which attempts to relate the turbulent shear stress, essentially a turbulent fluctuation phenomena, to the mean properties of the fluid through a fictitious "mixing length" (2). This theory has given reasonably good results in incompressible problems for determining the spread of momentum. However, in the consideration of a turbulent compressible flow, it does not seem logical to use such a representation, since the compressible turbulent equations of motion cannot be derived to give the same form for the turbulent shear stress as the incompressible equations.

For this reason, a simple form for the turbulent shear stress is used in this paper instead of the Prandtl form,

$$\tau = \varepsilon \frac{\partial u}{\partial r} \tag{23}$$

In Equation 23, e can be referred to as a turbulent viscosity coefficient and u is the mean velocity of the flow. Some attempt must be made now to express e in terms of u, r_o, and r_i only so that the equations derived in Section 3 may be solved. Suppose that e can be broken into a density dependent term and a geometrically dependent term. The simplest way to do this is to say

$$e = \rho \epsilon \tag{24}$$

where ϵ can be considered to be a turbulent kinematic viscosity coefficient. It is assumed to vary only with x as suggested by Reichardt (4) who reached this conclusion through the analysis of many incompressible experimental data. Therefore ϵ is assumed to be proportional to the width of the mixing region, which is only a function of x. The shear stress is then given by

Core Region:

$$\tau = \rho K (r_o - r_i) \frac{\partial u}{\partial r} \tag{25a}$$

Developed Region:

$$\tau = \rho K r_o \frac{\partial u}{\partial r} \tag{25b}$$

The quantity K is then experimentally determined proportionality constant of the type that usually appears in semi-empirical analyses and has the dimensions of a velocity.

E. Solution of the Equations

Core Region:

It is now possible to express Equations 11 and 13 in terms of only the two dependent variables r_i and r_o. Substitution of Equation 18 for ρ and Equation 25a for τ gives

$$\frac{\rho_1 u_1^2 R_i^2}{2} + \int_{R_i}^{R_o} \left\{ \frac{\rho_1 - \rho_2}{u_1^2} + \rho_2 \right\} u^2 r \, dr = m \tag{26}$$

and

$$\left.\begin{aligned} &\frac{\rho_1 u_1^2}{4} \frac{\partial R_i^2}{\partial x} + \frac{\partial}{\partial x} \int_{R_i}^{\frac{R_o+R_i}{2}} \left\{ \frac{\rho_1 - \rho_2}{u_1^2} u^2 + \rho_2 \right\} u^2 r \, dr \\ &\quad - \frac{u}{2} \frac{\partial}{\partial x} \int_{R_i}^{\frac{R_o+R_i}{2}} \left\{ \frac{\rho_1 - \rho_2}{u_1^2} u^2 + \rho_2 \right\} u r \, dr \\ &\quad = -\left[\rho_1 + 3\rho_2 \right] \frac{\pi u_1 K}{16} (R_o + R_i) \end{aligned}\right\} \tag{27}$$

The right side of equation 27 is obtained by evaluating in Equation 25a at $r = \frac{r_o + r_i}{2}$ from Equation 6.

The integrals in Equations 26 and 27 can be evaluated by ordinary methods after substitution for u by Equation 6. The evaluated integrals and both equations can be seen to involve only the variables r_o and r_i. Upon reduction, the non-dimensional equations become

$$\frac{\rho_1}{\rho_2} = R_o^2 \left\{ a \left(\frac{\rho_1}{\rho_2} - 1 \right) + b \right\} + R_o R_i \left\{ c \left(\frac{\rho_1}{\rho_2} - 1 \right) + d \right\} + R_i^2 \left\{ \frac{\rho_1}{\rho_2} - f \left(\frac{\rho_1}{\rho_2} - 1 \right) - g \right\} \tag{28}$$

$$\frac{dR_o^2}{dX} \left\{ \frac{h}{4} \left(\frac{\rho_1}{\rho_2} - 1 \right) + j \right\} + \frac{d(R_o R_i)}{dX} \left\{ \frac{k}{2} \left(\frac{\rho_1}{\rho_2} - 1 \right) + 2l \right\} + \frac{dR_i^2}{dX} \left\{ \frac{\rho_1}{\rho_2} - \frac{m}{4} \left(\frac{\rho_1}{\rho_2} - 1 \right) - n \right\} = -\left[\frac{\rho_1}{\rho_2} + 3 \right] \frac{\pi}{4} \frac{K}{u_1} (R_o + R_i) \tag{29}$$

where $R_o = \frac{r_o}{r_1}$, $R_i = \frac{r_i}{r_1}$, $X = \frac{x}{r_1}$. The lettered constants are given in Appendix II. Equations 28 and 29 are similar in form to those derived by Squire and Trouncer who give an intricate method of solution for R_o and R_i. This method is not followed, however, since it was felt that a graphical integration would yield results more quickly.

The method used to solve Equations 28 and 29 is as follows:

Equation 28 was solved for R_o in terms of R_i and also differentiated with respect to X to give $\frac{dR_o}{dX}$. R_o, $\frac{dR_o}{dX}$, and $\frac{dR_o}{dX}$ were substituted into Equation 29 and, upon reduction, an expression relating R_i and X was found,

$$f(R_i)\frac{dR_i}{dX} = \frac{K}{a_1} \tag{30}$$

where f (R_i) is a function of R_i and ρ_1/ρ_2 only (See Appendix II). Using the boundary condition at the jet exit

$$R_i = 1 \text{ at } X = 0$$

Equation 30 can be integrated to give

$$\int_1^{R_i} f(R_i)\,dR_i = \int_0^X \frac{K}{a_1}\,dX = \frac{K}{a_1}X \tag{31}$$

The function f (R_i) was calculated for values of R_i varying between 1 at the nozzle exit and 0 at the end of the potential core and for various density ratio values, $2.425 \geq \rho_1/\rho_2 \geq .1667$. Values of $\frac{K}{a_1}X$ corresponding to the chosen R_i and ρ_1/ρ_2 values were then calculated graphically and R_o was calculated from Equation 28.

Figure 4 shows the calculated R_o and R_i values as functions of $\frac{K}{a_1}X$ for the ρ_1/ρ_2 range. Figure 5 gives the length of the potential core as a function of density ratio ρ_1/ρ_2.

Developed Region:

Substitution of Equation 18 for ρ and Equation 24b for τ into Equations 14 and 15 gives

$$\int_0^{R_0}\left\{\frac{\rho_1-\rho_2}{u_1^2}u^2+\rho_2\right\}u^2 n\,dn = m \tag{32}$$

and

$$\left.\begin{aligned}&\frac{\partial}{\partial x}\int_0^{R_0\sqrt{2}}\left\{\frac{\rho_1-\rho_2}{2u_1^2}u^2+\rho_2\right\}u^2 n\,dn\\&\quad-\frac{u_c}{2}\frac{\partial}{\partial x}\int_0^{R_0\sqrt{2}}\left\{\frac{\rho_1-\rho_2}{u_1^2}u^2+\rho_2\right\}u\,n\,dn\\&\quad=-\left[\frac{\rho_1-\rho_2}{u_1^2}\frac{u_c^2}{4}+\rho_2\right]\frac{\pi}{4}\kappa u_c R_0\end{aligned}\right\} \tag{33}$$

The integrals in Equations 32 and 33 again can be evaluated when substitution for u is made with Equation 7. The non-dimensional equations become

$$R_0^2=\frac{\rho_1/\rho_2}{\left(\rho_1/\rho_2-1\right)\frac{a_1}{8}U^4+\frac{b_1}{2}U^2} \tag{34}$$

$$\begin{aligned}&\frac{dR_0^2}{dX}\left\{\frac{U^4\left(\frac{\rho_1}{\rho_2}-1\right)}{16}(c_1-d_1)+\frac{U^2}{4}(f_1-g_1)\right\}\\&+R_0^2\frac{dU}{dX}\left\{\frac{U^3\left(\frac{\rho_1}{\rho_2}-1\right)}{16}(4c_1-3d_1)+\frac{U}{4}(2f_1-g_1)\right\}\\&\qquad=-\left[\left(\frac{\rho_1}{\rho_2}-1\right)\frac{U^2}{4}+1\right]\frac{\pi}{4}\frac{\kappa}{u_1}UR_0\end{aligned} \tag{35}$$

where $R_0=\frac{r_0}{r_1}$, $U=\frac{u_c}{u_1}$, $X=\frac{x}{r_1}$. The lettered constants are given in Appendix II. Substitution into Equation 35 for R_0 from Equation 34 results in an expression involving only U and X,

$$g(U)\frac{dU}{dX}=\frac{\kappa}{u_1} \tag{36}$$

where g (U) is a function of U and ρ_1/ρ_2 only (See Appendix II). The

boundary condition that

$$U = 1 \text{ at } X = X_c,$$

where X_c is the length of the potential core, is then employed to integrate Equation 36

$$\int_1^U g(U)\,dU = \int_{x_c}^{x} \frac{\kappa}{u_1}\,dx = \frac{\kappa}{u_1}(x - x_c) \qquad (37)$$

The function g (U) was calculated for values of U and ρ_1/ρ_a in the following ranges:

$$1.00 \geq U \geq .125$$

$$2.425 \geq \rho_1/\rho_a \geq 1.667$$

Values of $\frac{\kappa}{u_1} X$ corresponding to U were calculated graphically according to Equation 37. R_o values were calculated from Equation 34.

The variation of axial velocity is plotted in Figure 6 for different values of ρ_1/ρ_a. Figure 7 shows the spread of the jet as a function of $\frac{\kappa}{u_1} X$ for various density ratios.

Solution of a Particular Mixing Problem:

Figures 8 and 9 present crossplots of Figures 4, 6, and 7 showing the spread of the jet and the decay of velocity along the axis respectively as a function of ρ/ρ_a for various $\frac{x}{d}$, K values. When it is desired to predict the characteristics of a jet of known density, or temperature, assuming the pressure to be constant, exhausting into a still medium of known density, Figures 5, 8, and 9 are easily used to find the potential core length, the jet boundaries, and the velocity decay on the axis. Equation 6 or Equation 7, the cosine velocity variations, will then give the velocity at any point in the jet.

It is the purpose of this paper to discuss the effect of density upon a jet discharging into still air only. However, it seems that the case of an external stream velocity not equal to zero could be taken into account quite easily by the method given by Küchemann and Weber(12) involving a change of the coordinate system.

Effect of Density Variation Upon Jet Characteristics:

Qualitatively, the effect of varying density upon the characteristics of a jet spreading into a free stream of zero velocity can be seen in Figures 6 and 7. It is noticed that the potential core becomes longer as the density ratio increases (Figure 5). A hot jet, low ρ/ρ_a values, not only has a shorter potential core, but its centerline velocity also drops off much faster with axial distance than a cold jet. This is in general agreement with Corrsin and Uberoi(13) who observed that a warm jet spreads faster and, therefore, its centerline velocity decreases more

rapidly than a cool jet.

The spread of the jet boundaries, R_i and R_o, is interesting when it is noticed that until an axial distance of about $\frac{K}{\alpha_o} X = .055$ is reached the hottest jet, $\rho_i/\rho_a = .1667$, has the least outward spread, although its inward spread is the most rapid. However, after $\frac{K}{\alpha_o} X = .067$ this jet has the most rapid outward spread. These effects can be explained, qualitatively, as follows:

Consider a hot and a cold jet of equal initial velocity exhausting from nozzles of equal radii into surroundings of equal density. The total momentum flux of a jet, which will be proportional to ρu^2, will be less for the hot than for the cold jet. For this reason, a comparitively small amount of momentum transfer will be needed in the hot jet case to destroy the potential core completely. Consequently, a smaller amount of outside air is needed to be entrained, causing less outward spread for the hot jet in the core region. After the core has disappeared, the velocity on the axis decays more rapidly in the hot jet, also because of the reason just given. However, the conservation of momentum condition must be preserved thus causing the outer boundary of the hot jet to spread rapidly after the core is destroyed.

The Mixing Parameter, $\frac{K}{u_j}$:

Until now, the results of the calculations have been presented in terms of $\frac{K}{\alpha_o} X$, K being the proportionality constant in the shear stress representation, Equation 25. At first, it appears that the absolute velocity of the jet exhausting from the nozzle, u_j, has an important influence upon the axial dimension. However, experimental results(12)

show quite clearly that the characteristics of the jet depend primarily upon the ratio of the extrenal stream velocity to the jet exit velocity and only negligibly, if at all, upon the absolute velocity of either. Therefore, since this analysis was derived for the free jet case; i.e., for the particular velocity ratio of zero, neither the velocity nor any velocity ratio should enter into the determination of the jet characteristics. For this reason, it is believed that the quantity $\frac{K}{u_1}$ should be considered as the empirical constant instead of K alone.

A value of $\frac{K}{u_1}$ was determined from the data of Pabst(14), which was taken at a density ratio $\rho_1/\rho_2 = .455$. A value of $\frac{K}{u_1} = .0038$ was found to match the length of the potential core, which he found to be 12.0 nozzle radii. A comparison between Pabst's velocity decay data and the velocity decay predicted by this analysis (Figure 9) using $\frac{K}{u_1} = .0038$ is given in Figure 10. The agreement is reasonably good up to the limit of the experiment which is about 25 nozzle diameters downstream.

There is, however, an indication that $\frac{K}{u_1}$ varies with density ratio ρ_1/ρ_2. Data taken by Corrsin(15) at a density ratio $\rho_1/\rho_2 = .965$ result in a $\frac{K}{u_1}$ value of .0059 when the theory is matched with experiment at the end of the potential core.

The results of early experiments at this laboratory (11) are shown in Figure 11 for the case of an extremely cold jet, $\rho_1/\rho_2 = 2.30$. When evaluated at the end of the potential core, as defined by a sudden change in center line velocity, $\frac{K}{u_1} = .0033$. The theoretical agreement with velocity decay downstream is then fairly good; however, the number of experimental data are not sufficient for an accurate evaluation. It should be noted that the jet exit Mach number was approximately 2.6 in these experiments and weak shock disturbances present in the initial

portion of the jet might have changed the length of the potential core from its ideal value. It is believed, though, that shock effects were small and that the value of $\frac{\kappa}{a_1} = .0033$ is reasonably accurate.

Therefore, there appears to be a variation in the mixing parameter $\frac{\kappa}{a_1}$ with density ratio, which was not accounted for in the development of the theory being presented. A systematic experimental determination of $\frac{\kappa}{a_1}$ will be a part of future tests conducted at this laboratory.

References

1. W. Tollmien, Berechnung der Turbulenten Ausbreitungs vorgänge, ZAMM 4, 468, 1926. Translated as N.A.C.A. T.M. 1085, 1945.
2. S. Goldstein, Modern Developments in Fluid Dynamics, Volume I, Oxford, 1938.
3. A. M. Kuethe, Investigation of the Turbulent Mixing Regions Formed by Jets, J. Appl. Mech., 2, 87-95, 1935.
4. H. Reichardt, Über eine Neue Theorie der Freien Turbulenz, ZAMM 21, 257-264, 1941.
5. H. B. Squire and J. Trouncer, Round Jets in a General Stream, R. & M. No. 1974, British A.R.C., 1944.
6. W. Forstall, Jr. and A. H. Shapiro, Momentum and Mass Transfer in Coaxial Gas Jets, J. Appl. Mech., 17, 399-408, 1950.
7. S. S. Pai, Axially Symmetrical Jet Mixing of a Compressible Fluid, Quart. of Appl. Math., 10, 141-148, 1952.
8. W. Szablewski, Die Ausbreitung eines Heissluftstrahles in Bewegter Luft, GDC/246, 1946. Translated as N.A.C.A. T.M. 1288, 1950.
9. A. Kivnick, Application of the Reichardt Hypothesis to the Transport of Momentum and Mass in Coaxial Jets, Tech. Rep. No. CML-2, Engineering Experiment Station, University of Illinois, 1952.
10. A. A. Townsend, Momentum and Energy Diffusion in the Turbulent Wake of a Cylinder, Proc. Roy. Soc., 197A, 124-140, 1949.
11. E. T. Pitkin, An Experimental Investigation of an Axially Symmetric Supersonic Jet Mixing with Free Air, Princeton University Aero. Eng'g. Lab. Report No. 243 , 1953.

12. D. Kuchemann and J. Weber, Aerodynamics of Propulsion, Chapter 10, McGraw-Hill, 1953.

13. S. Corrsin and M. S. Uberoi, Further Experiments on the Flow and Heat Transfer in a Heated Turbulent Air Jet, N. A. C. A. T. N. 1865, 1949. Also available as N.A.C.A. Report No. 998, 1950.

14. O. Parst, Die Ausbreitung heisser Gasstrahlen in Bewegter Luft, I. Teil - Versuche im Kerngebiet, Deutsche Luftfahrtforschung., Untersuchs-Mitteilungen, No. 6004, II. Teil., Untersuchs-Mitteilungen, No. 6007, 1944.

15. S. Corrsin, Investigation of Flow in an Axially Symmetrical Heated Jet of Air, N.A.C.A. A.C.R. 3L23, 1943.

Appendix I Solution of the Mixing Problem Using a Linear Velocity Profile and the Crocco Integral for Density Variation

Equation 16 is an expression of the Crocco integral type and is an exact solution of the general energy equation in the Prandtl number of the flow is assumed to be unity and if the pressure is assumed to be constant. It would be desirable to represent the density variation in a jet by such an expression instead of the approximation given by Equation 18. Equation 16 can be rewritten as

$$\frac{1}{\rho} = \alpha + \beta u - \frac{u^2}{2c_0} \tag{I.1}$$

where α and β can be determined by the boundary conditions of the given jet.

The applicability of the method of solution presented in this paper depends upon the possibility of being able to express integrals of the form

$$\int_0^\delta \rho u^2 r\, dr \tag{I.2}$$

as algebraic functions of their limits, since the limits always contain at least one of the unknowns of the problem. That is, expressions similar to Equation I.2 must be integrable. The assumption of the cosine shaped velocity profile eliminates the use of Equation I.1 as a density variation because of the resulting complicated form of the integrand in Equation I.2 when substitution for u is made.

An interesting calculation has been made by Fitkin(11) at this laboratory. He employed a linear velocity variation and recalculated

the incompressible problem of Squire and Trouncer for the one case of no external velocity, obtaining results almost identical with theirs. This shows in part that the assumed velocity profile is of little importance in the method of solution, a result typical of analyses employing integral equations. The velocity profiles used by Pitkin are

Core Region:

$$u = u_i \left\{ \frac{r_o - r}{r_o - r_i} \right\} \tag{I.3}$$

Developed Region:

$$u = u_c \left\{ 1 - \frac{r}{r_o} \right\} \tag{I.4}$$

Now, if it is assumed that linear profiles can be used in the compressible jet case without causing an appreciable change in results (a method of checking this assumption would be to repeat the analysis presented in this paper using linear profiles and compare calculated results), the problem may be solved using the more exact density expression, Equation I.1. This can be seen by substituting Equations I.1 and I.3 into Equation I.2 which gives

$$\int_0^{\delta} \frac{u_i^2 \left(\frac{r_o - r}{r_o - r_i} \right)^2}{\alpha + \beta u - \frac{u^2}{2 c_o}} r \, dr \tag{I.5}$$

Upon reduction, Equation I.5 may be split into 3 integrals, the most complicated being of the form

$$\int_0^{\delta} \frac{r^2}{\alpha_1 + \beta_1 r + r^2} \, dr \tag{I.6}$$

Equation I.6 is rational and may be evaluated easily, although tediously.

Appendix II Constants and Functions Appearing in Equations

Equation 28):

$$a = \frac{35}{128} - \frac{16}{9\pi^2} \qquad b = \frac{3}{8} - \frac{2}{\pi^2}$$

$$c = \frac{32}{9\pi^2} \qquad d = \frac{4}{\pi^2}$$

$$e = \frac{35}{128} + \frac{16}{9\pi^2} \qquad g = \frac{3}{8} + \frac{2}{\pi^2}$$

Equation 29):

$$h = \frac{15}{64} + \frac{3}{2\pi} - \frac{1613}{384\pi^2} \qquad j = \frac{1}{16} + \frac{1}{2\pi} - \frac{5}{4\pi^2}$$

$$k = \frac{15}{64} + \frac{1613}{384\pi^2} \qquad l = \frac{1}{16} + \frac{5}{4\pi^2}$$

$$m = \frac{15}{64} + \frac{3}{2\pi} + \frac{1613}{384\pi^2} \qquad n = \frac{3}{16} + \frac{1}{2\pi} + \frac{5}{4\pi^2}$$

Equation 30):

$$f(R_i) = \frac{(B - \frac{AF}{E})(R_o + R_i Z) + 2(C - \frac{AG}{E})R_i}{(R_o + R_i)D}$$

where:

$$R_o = -\frac{FR_i \pm \sqrt{F^2R_i^2 - 4E(GR_i^2 - H)}}{2E}$$

$$Z = -\frac{F}{2E} + \frac{R_i(2F^2 - 8EG)}{4E\sqrt{F^2R_i^2 - 4E(GR_i^2 - H)}}$$

$$A = \frac{b}{4}\left(\frac{\rho}{\rho_a} - 1\right) + j \qquad B = \frac{d}{2}\left(\frac{\rho}{\rho_a} - 1\right) + 2l$$

$$C = \frac{\rho}{\rho_a} - \frac{\pi^2}{4}\left(\frac{\rho}{\rho_a} - 1\right) - g \qquad D = -\left[\frac{\rho}{\rho_a} + 3\right]\frac{\pi^2}{4}$$

$$E = a\left(\frac{\rho}{\rho_a} - 1\right) + b \qquad F = e\left(\frac{\rho}{\rho_a} - 1\right) + d$$

$$G = \frac{\rho}{\rho_a} - f\left(\frac{\rho}{\rho_a} - 1\right) - g \qquad H = \rho_i/\rho_a$$

Note: lower case letters refer to constants listed for Equations 28 and 29

Equation 34):

$$a_1 = \frac{25}{16} - \frac{128}{9\pi^2} \qquad b_1 = \frac{3}{4} - \frac{4}{\pi^2}$$

Equation 35):

$$c_1 = \frac{35}{64} + \frac{10}{3\pi} - \frac{320}{36\pi^2} \qquad d_1 = \frac{5}{16} + \frac{11}{6\pi} - \frac{163}{36\pi^2}$$

$$f_1 = \frac{3}{16} + \frac{1}{\pi} - \frac{2}{4\pi^2} \qquad g_1 = \frac{1}{8} + \frac{1}{2\pi} - \frac{1}{\pi^2}$$

Equation 36):

$$g(U) = \frac{A_1 U^4 + B_1 U^2 + C_1}{(D_1 U^3 + E_1 U)[F_1 U^2 + G_1]^{3/2}}$$

where:

$$A_1 = \frac{\rho_1}{\rho_2}\left(\frac{\rho_1}{\rho_2} - 1\right)^2 \frac{a_1 d_1}{512}$$

$$B_1 = \frac{\rho_1}{\rho_2}\left(\frac{\rho_1}{\rho_2} - 1\right) \frac{26 c_1 - 6 d_1 - 2 a_1 f_1 + 32 g_1}{128}$$

$$C_1 = \frac{\rho_1}{\rho_2} \frac{6 g_1}{32}$$

$$D_1 = -\sqrt{\frac{\rho_1}{\rho_2}\left(\frac{\rho_1}{\rho_2} - 1\right)} \frac{\pi}{16\sqrt{2}}$$

$$E_1 = -\sqrt{\frac{\rho_1}{\rho_2}} \frac{\pi}{4\sqrt{2}}$$

$$F_1 = \left(\frac{\rho_1}{\rho_2} - 1\right) \frac{a_1}{16}$$

$$G_1 = \frac{b_1}{4}$$

Note: lower case letters refer to constants listed for Equations 34 and 35.

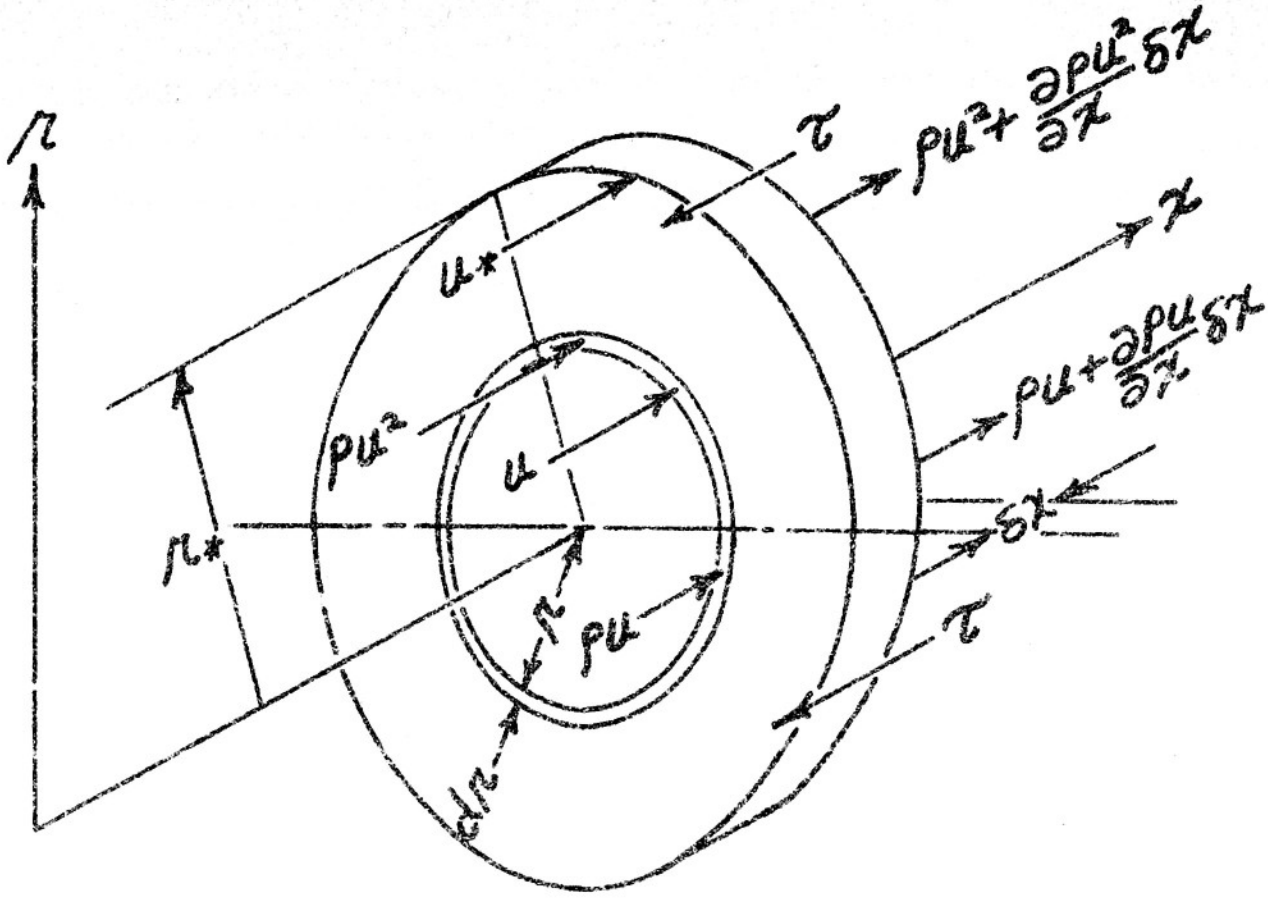

FIGURE 1.

ILLUSTRATION OF PROPERTIES OF A CIRCULAR DISK OF FLUID IN AXIAL SYMETRIC FLOW

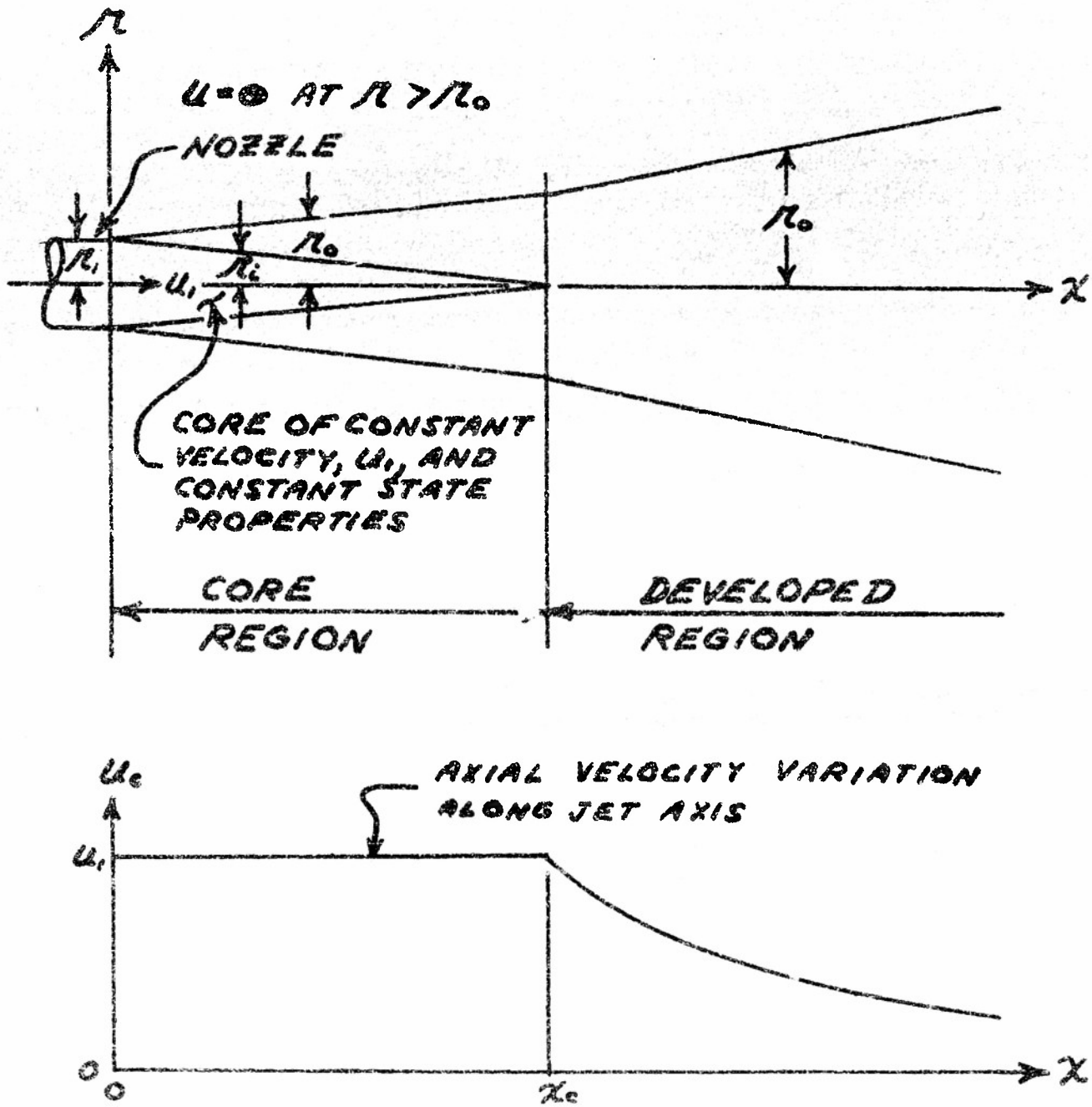

FIGURE 2.

STRUCTURE AND NOMENCLATURE OF FREE JET USED IN THE ANALYSIS

a. CORE REGION

$$u = \frac{u_1}{2}\left[1 - \cos \pi \left(\frac{r_o - r}{r_o - r_i}\right)\right]$$

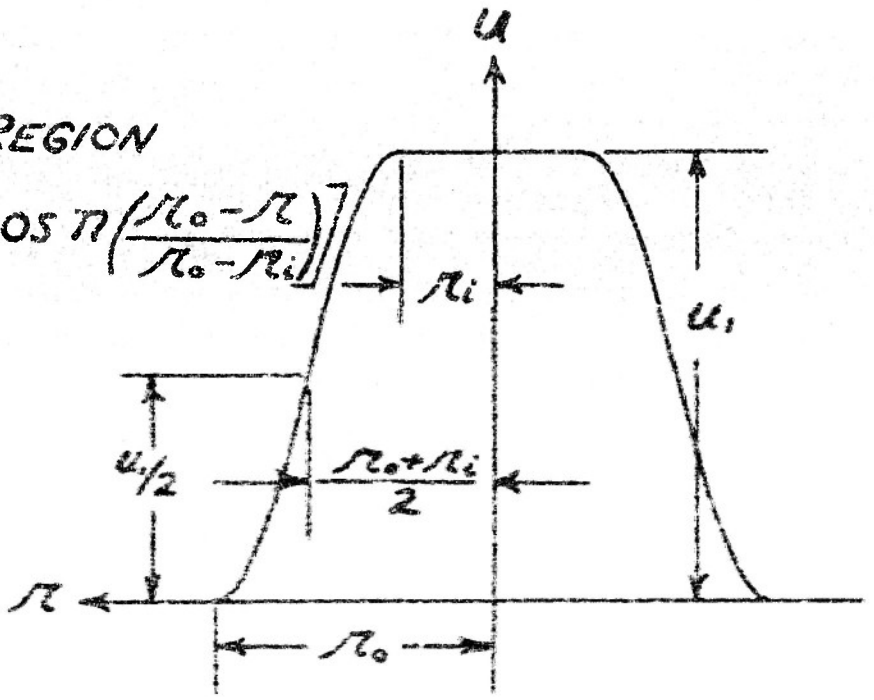

b. DEVELOPED REGION

$$u = \frac{u_c}{2}\left[1 + \cos \pi \frac{r}{r_o}\right]$$

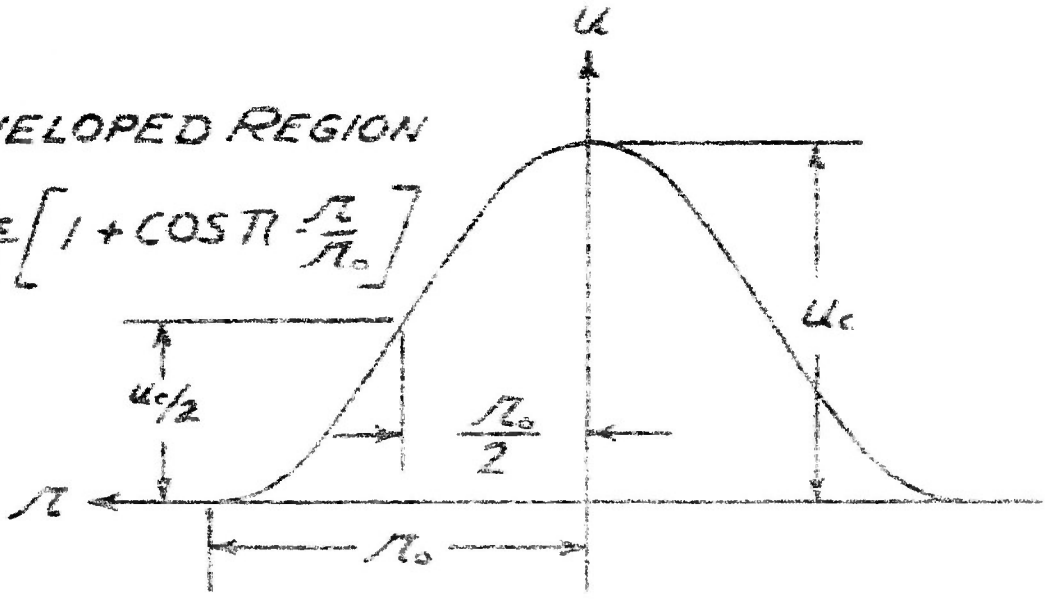

FIGURE 3.

ASSUMED VELOCITY PROFILES IN FREE JET

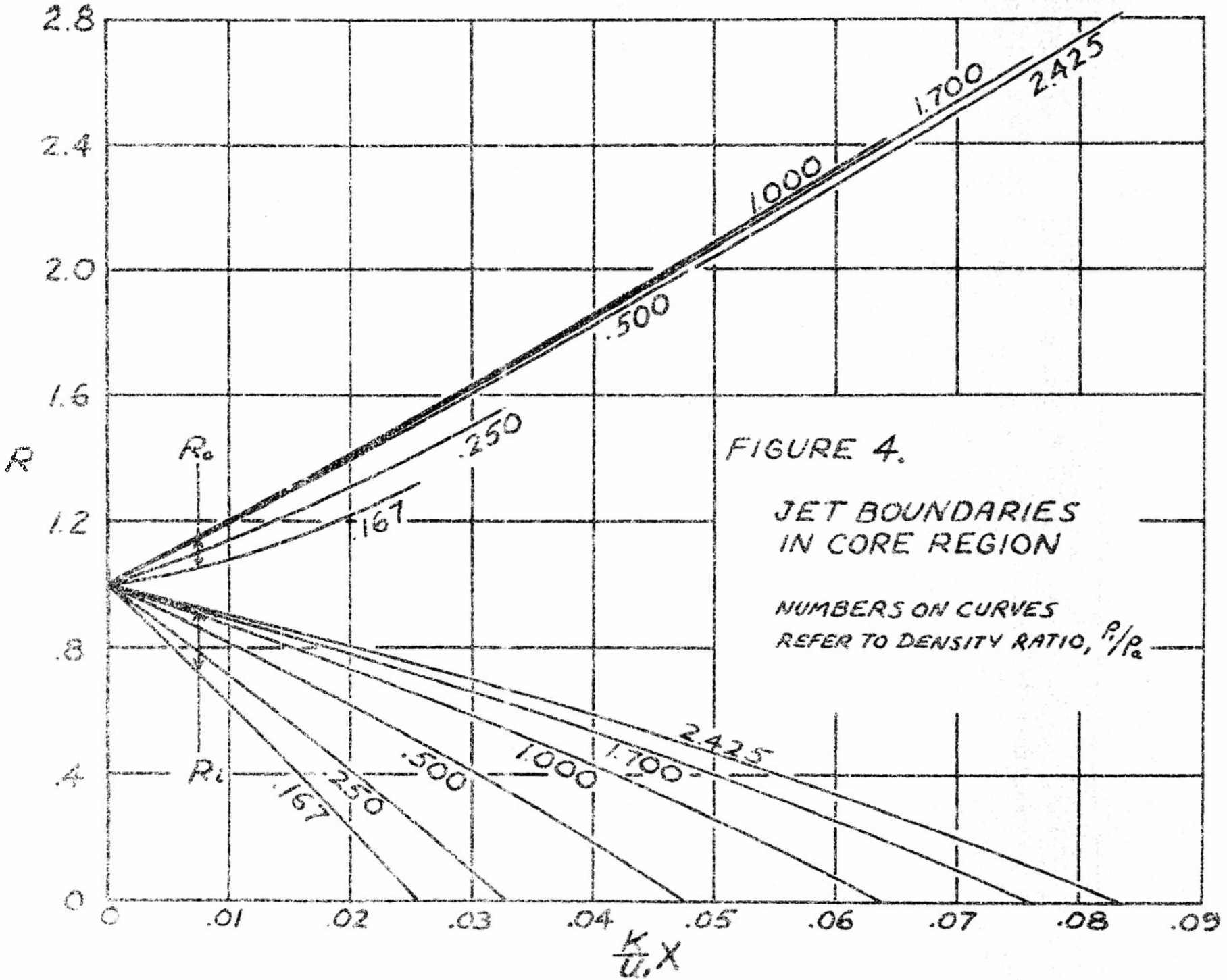
2.8
2.4
2.0
1.6
1.2
.8
.4
0
R
0
.01
.02
.03
.04
.05
.06
.07
.08
.09
K/U.X
Ro
Ri
1.700
2.425
1.000
.500
.250
.167
FIGURE 4.
JET BOUNDARIES IN CORE REGION
NUMBERS ON CURVES REFER TO DENSITY RATIO, ρi/ρo

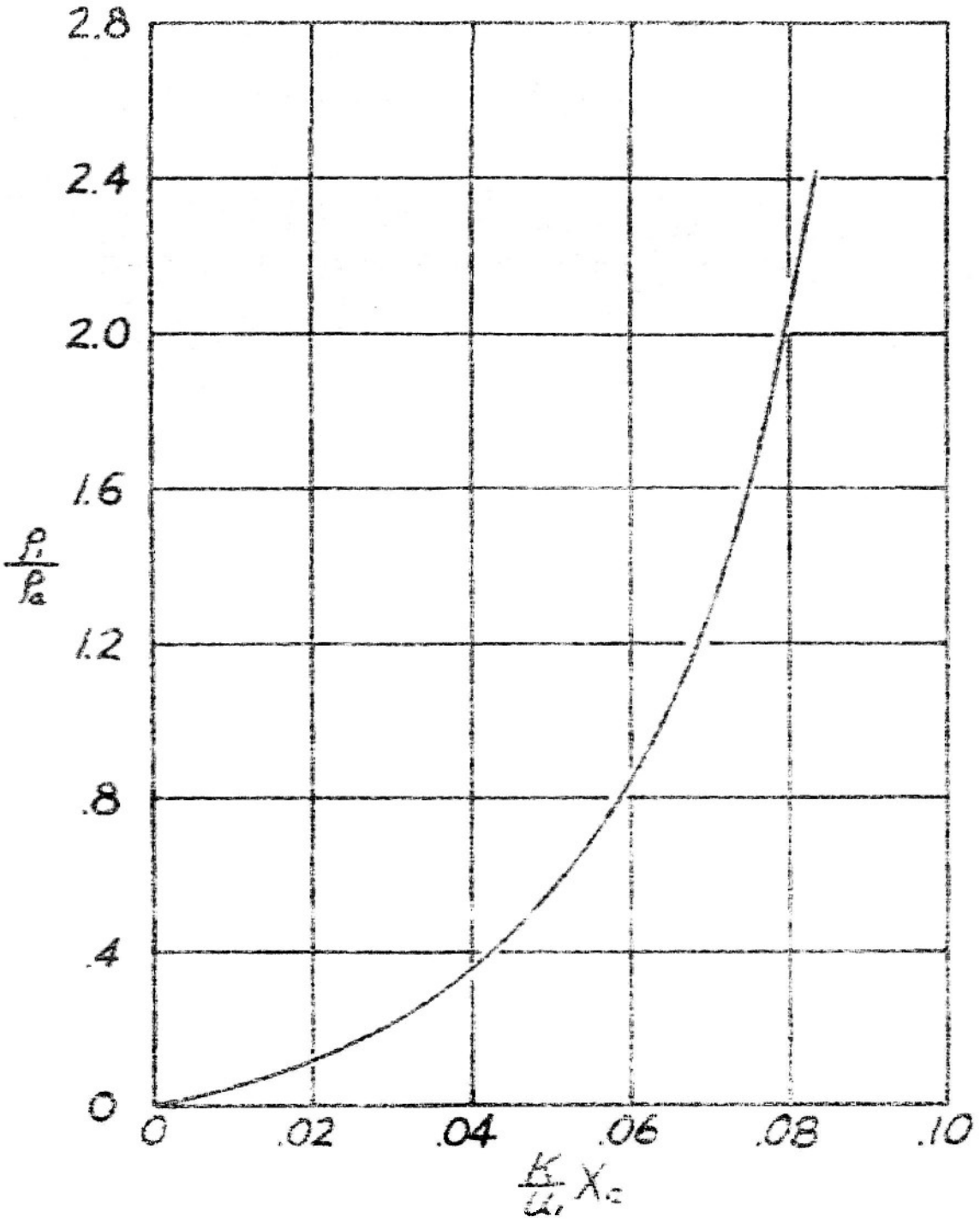

FIGURE 5.

LENGTH OF POTENTIAL CORE AS A FUNCTION OF DENSITY RATIO, ρ_1/ρ_a

FIGURE 6. DECAY OF CENTERLINE VELOCITY

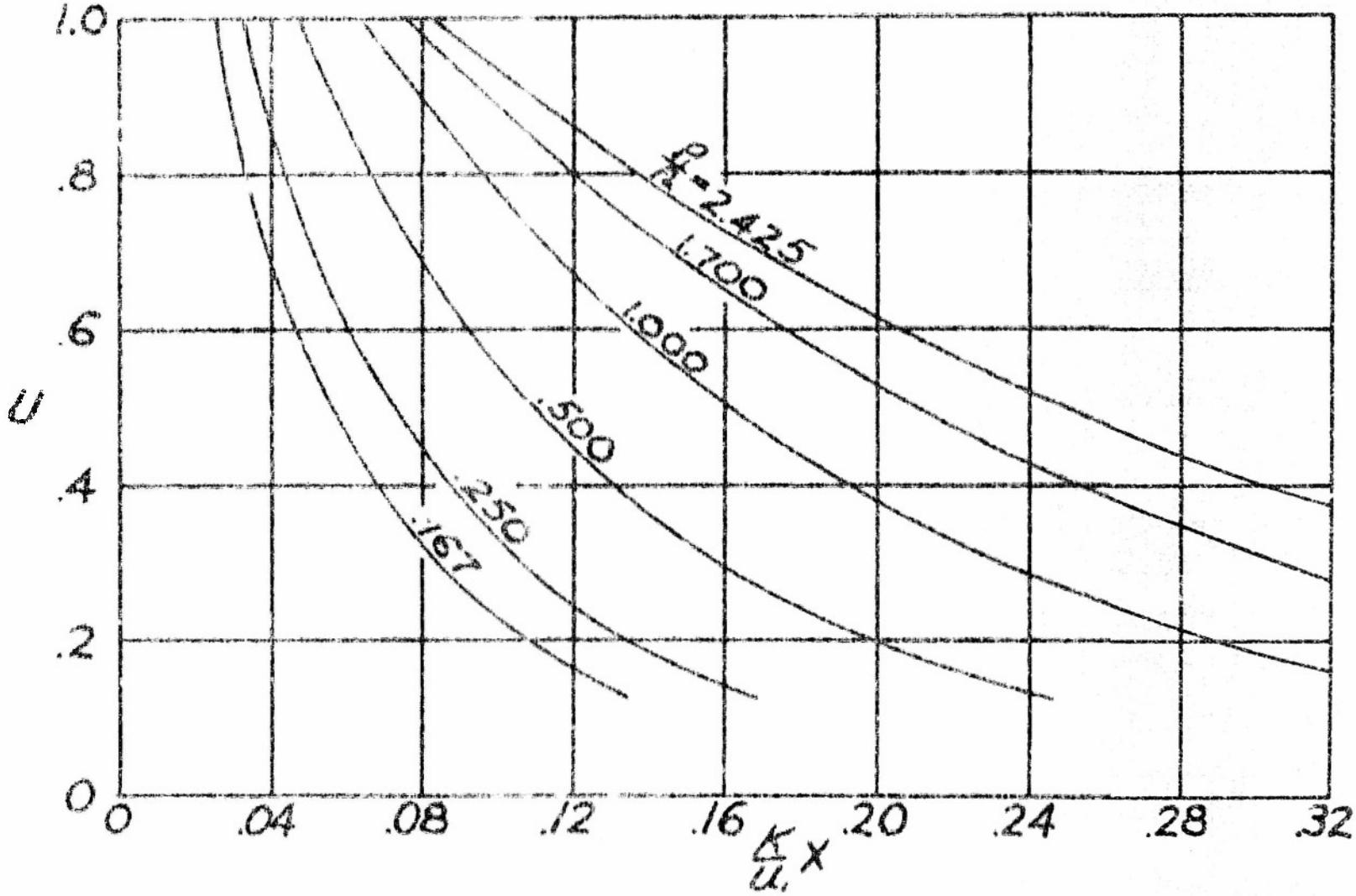

FIGURE 7.
JET BOUNDARIES

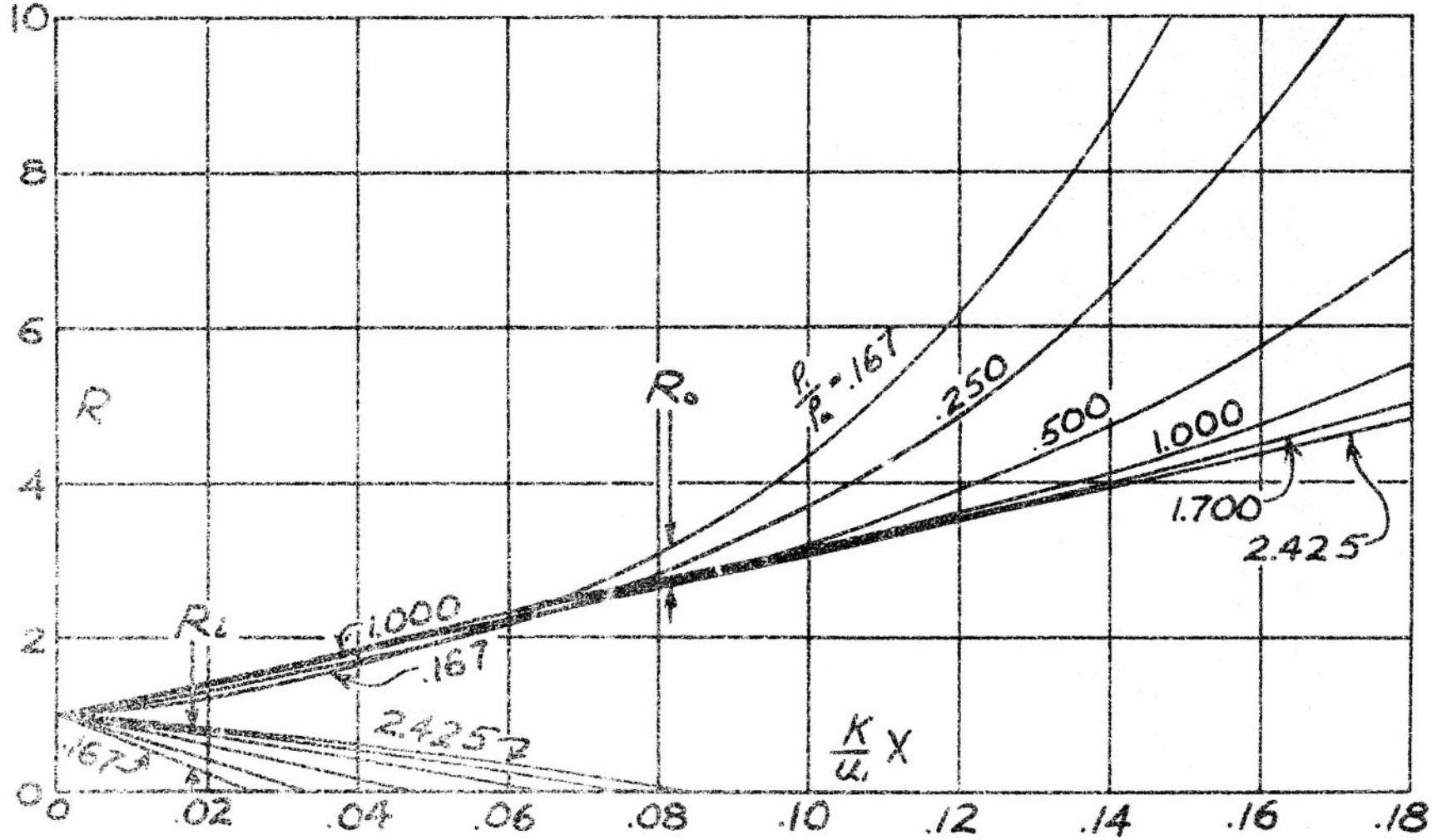

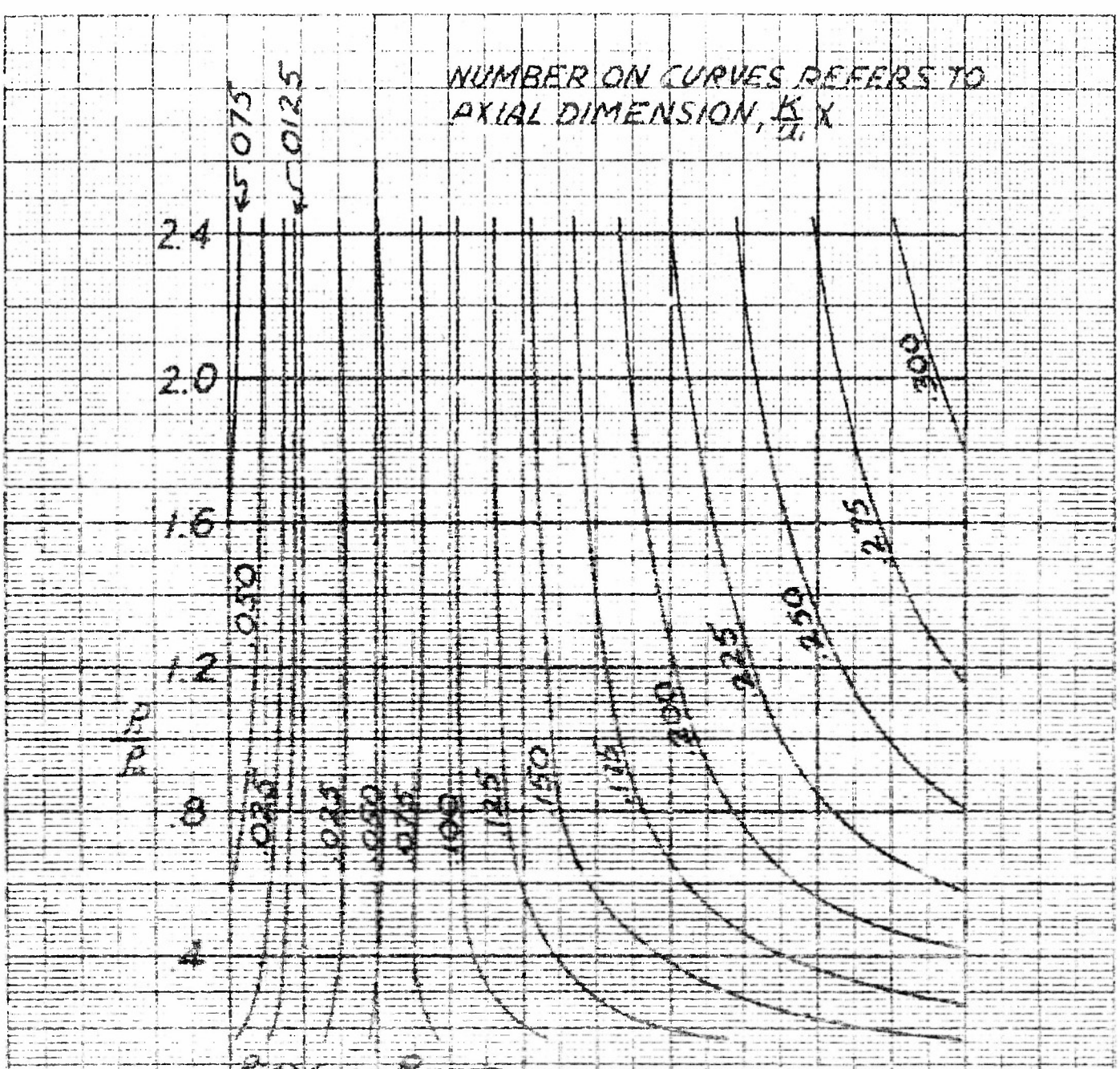

FIGURE 8.

JET BOUNDARIES AS FUNCTIONS OF DENSITY RATIO FOR VARIOUS DOWNSTREAM POSITIONS

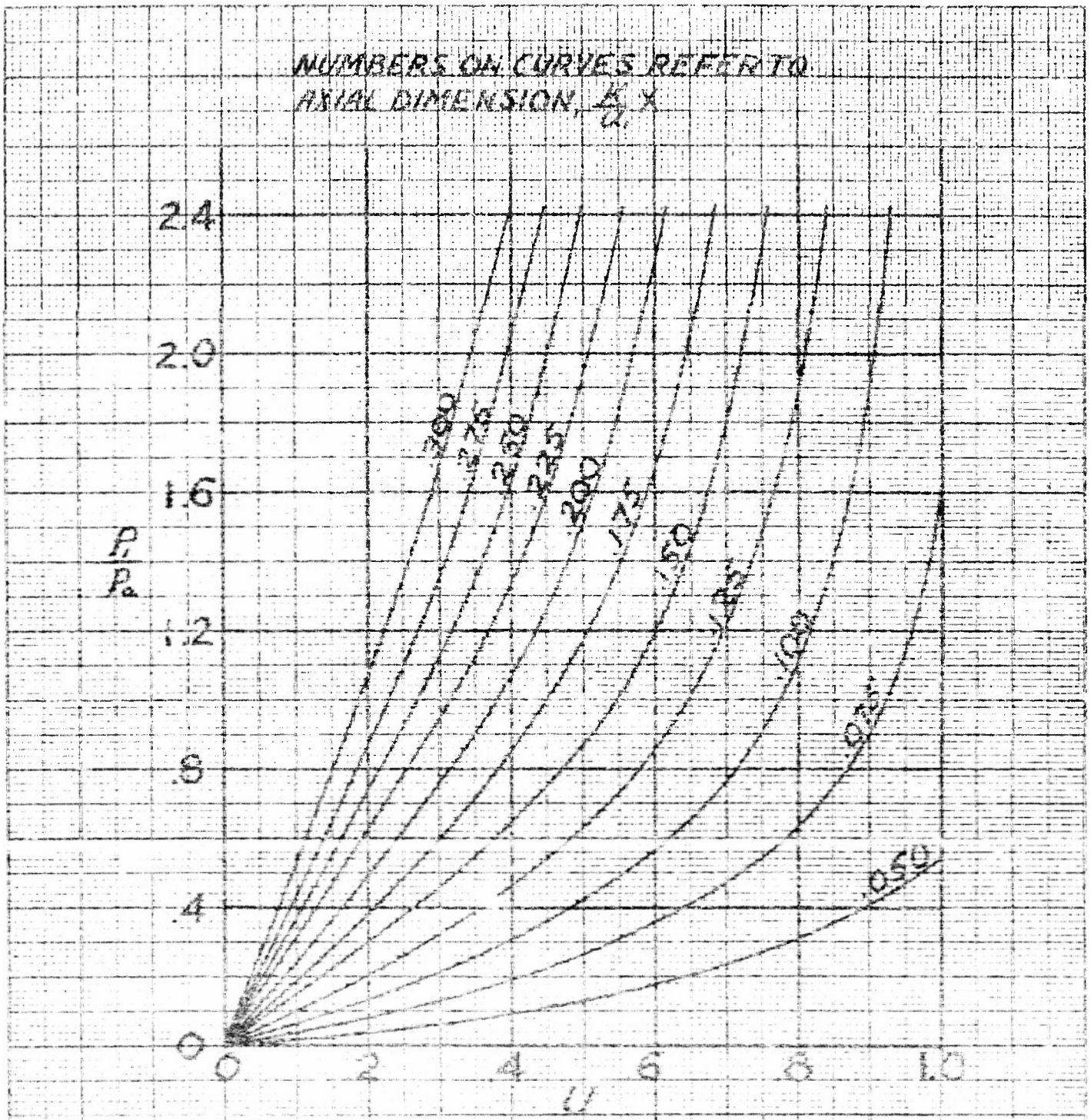

FIGURE 9.

CENTERLINE VELOCITY VARIATION AS FUNCTION OF DENSITY RATIO FOR VARIOUS DOWNSTREAM POSITIONS

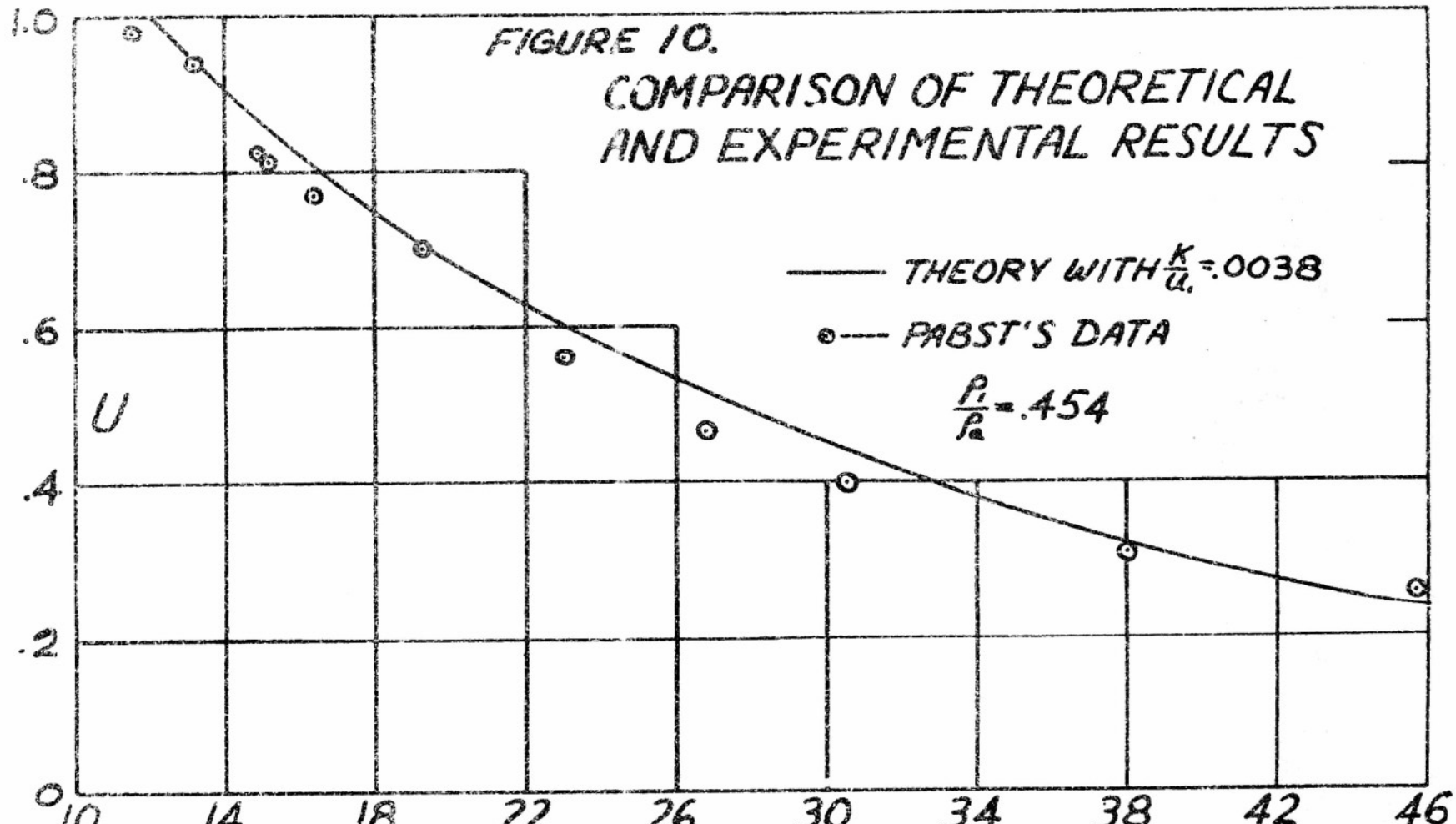
FIGURE 10.
COMPARISON OF THEORETICAL AND EXPERIMENTAL RESULTS
THEORY WITH $\frac{K}{u_1}$ = .0038
PABST'S DATA
$\frac{\rho_1}{\rho_2}$ = .454
U
X
1.0
.8
.6
.4
.2
0
10
14
18
22
26
30
34
38
42
46

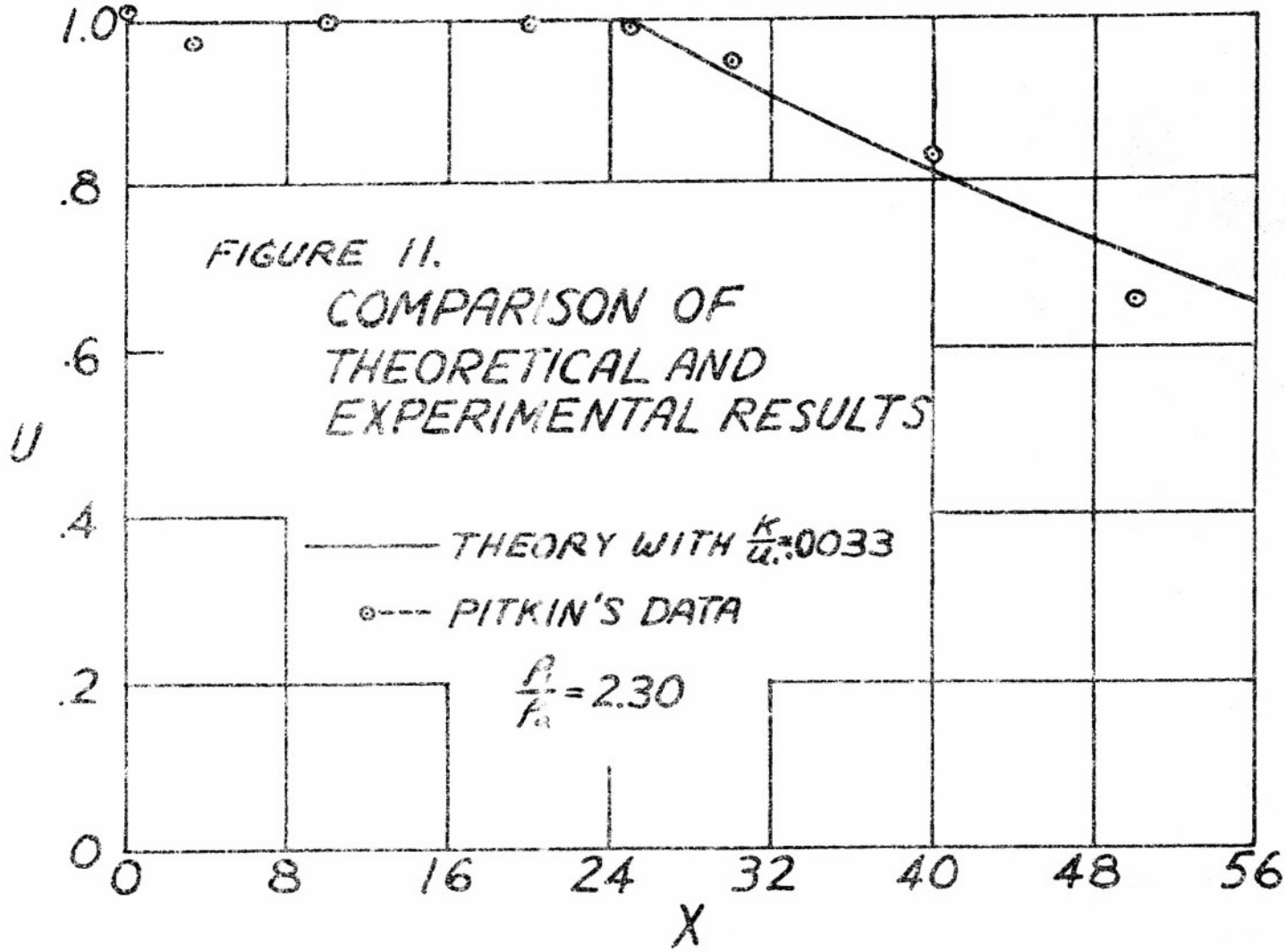
1.0
.8
.6
.4
.2
0
U
0
8
16
24
32
40
48
56
X
FIGURE 11.
COMPARISON OF
THEORETICAL AND
EXPERIMENTAL RESULTS
THEORY WITH $\frac{K}{u_*}$=.0033
PITKIN'S DATA
$\frac{\rho}{\rho_a}$=2.30